JOURNAL OF MATERIALS SCIENCE **38** (2003) 2063–2072

Oxidation of chromia forming molybdenum-tungsten based alloys

S. DILIBERTO, C. RAPIN, P. STEINMETZ, M. VILASI, P. BERTHOD
Laboratoire de Chimie du Solide Minéral—UMR CNRS 7555, Université Henri Poincare, BP 239, 54506 Vandoeuvre, France
E-mail: dilibert@sciences-univ-metz.fr

The oxidation behaviour of tungsten and molybdenum based, chromia-forming alloys prepared by powder sintering activated with group VIII metals has been investigated. The influences of the alloy composition, nature of the sintering agent and oxidation temperature have been studied. A good oxidation resistance is observed with palladium as sintering agent. This metal is rejected at the grain boundaries and allows a fast diffusion of chromium to the metal-oxide interface. Contrary to palladium, nickel leads to a catastrophic oxidation of the sample. The formation of a two-phase interface enriched in nickel leads to a non-protective oxide layer constituted with Cr_2O_3 and $NiWO_4$.

Catastrophic oxidation is observed when the refractory metals are oxidised into volatile oxides, i.e. in the case of the alloys with a high molybdenum content. Contrary to molybdenum, a high tungsten level leads to high oxidation resistance, even at temperature as high as 1300°C. In this latter case, alloys are two-phase: this result has led to the investigation of the ternary section of the Cr-Mo-W system at 1300°C.

1. Introduction

Many industrial applications require high-performance materials with good mechanical properties and high resistance to oxidation/corrosion at high temperatures. This is especially true in the glass industry, where metallic or ceramic materials suffer from high-temperature oxidation and corrosion by molten glass at temperatures up to 1200°C or higher. In most applications, good mechanical properties are also necessary.

As in other industrial fields, glass melting processes are evolving towards higher temperatures than those used classically. For example, due to changes in glass composition used to make insulation materials, temperature objectives for fiberglass processing can be as high as 1300°C. In this case, iron-, nickel- or cobalt-based alloys cannot be used, due to their drastic loss of mechanical properties above 1200°C.

Because of the need for high-temperature mechanical properties and resistance to molten glass corrosion, the development of refractory alloys based on tungsten and/or molybdenum seems to be relevant but the oxidation resistance of these metals is very bad, so that alloying them with elements which form stoichiometric protective oxide layers, is a necessity. Among the element which can be used for this purpose, aluminium or silicon must be excluded, because their oxides are very soluble in molten glass. Chromium is preferable, since chromia has a low solubility in most acidic glasses.

In the past, some authors have studied Mo- and/or W-based alloys containing chromium. Evans [1] was the first to describe a method of preparation of such alloys, with sintering of a powder mixture of the constituting elements containing an activating agent (palladium). Dzykovitch *et al*. [2] confirmed later that palladium is necessary to activate interdiffusion in the W-Cr binary system, probably because it temporarily forms limited quantities of a molten Cr-Pd phase. Lee and Simkovich [3–6] studied some compositions of Mo-Cr-Pd and Mo-W-Cr-Pd and showed that the combination of tungsten and molybdenum offers the best performance in high-temperature oxidation. They described the oxidation mechanism and claimed that the 19Cr-40Mo-40W-1Pd alloy displays excellent oxidation behaviour.

Nothing has been done on chromium-rich alloys, on the influence of the W/Mo ratio or on the nature of the sintering agent. These parameters have been studied here, with the main objective to find alloy compositions, which could satisfy requirements of resistance to high-temperature oxidation/corrosion. The methods of preparing of the chromium-rich Mo-W-Cr alloys, and their metallurgical structures have been presented elsewhere [7].

2. Experimental

2.1. Materials

Metal powders with characteristics given in Table I were supplied by CERAC. In order to limit the diffusion time, only micron size powder were used.

TABLE I Metallic powders used

Elements	Origin	Granulometry	Purity
Chromium	Cerac	−325 mesh	99.6%
Molybdenum	Cerac	−325 mesh	99.9%
Tungsten	Cerac	−325 mesh	99.5%
Palladium	Johnson Mattey	1–1.5 μm	99.95%
Nickel	Cerac	−325 mesh	99.9%
Ruthenium	Johnson Mattey	Sponge	>99%

2.2. Methods of fabrication

Preliminary to sintering, the elemental powders are weighed, then blended manually in an agate mortar to obtain a homogeneous mixture. High-pressure sintering was carried out with the use of a high-temperature furnace equipped with a 10 ton uniaxial press. The blended metal powders were introduced into a graphite die (Fig. 1), coated with boron nitride applied by spraying. Boron nitride works as a diffusion barrier between graphite and metallic powders, thus limiting metallic carbide formation.

The experimental sequence used is shown in Fig. 2, which plots the pressure and temperature with time. In the first part of the experiment, the sample was slowly heated under a dynamic primary vacuum. When the temperature reached 800°C, argon was introduced to the furnace (10^5 Pa), and a 27 MPa pressure was applied to obtain a non-porous sintered sample [7].

The structure of the alloys prepared by this sintering technique have been described in another paper published previously [7]

All compositions in this paper are given in weight percent.

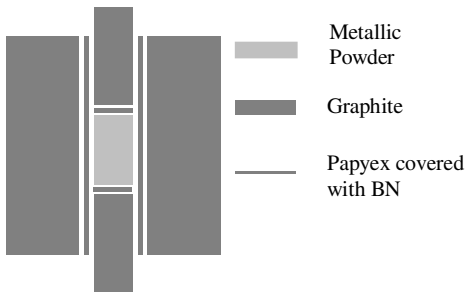

Figure 1 Scheme of graphite die.

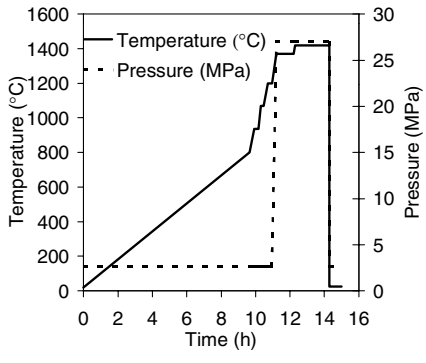

Figure 2 Temperature and pressure traces used to synthetise alloys.

2.3. Study of the oxidation behaviour of the alloys: experimental setup

Oxidation experiments have been conducted in a SETARAM B60 type automatic-recording balance (sensitivity 0.1 mg). A $1 \times 1 \times 0.3$ mm sample, polished at grit 1200 SiC-paper is hung in the hot zone of the thermobalance furnace by a platinum wire. Dry air is then introduced into the reaction chamber at 1 atm, with a flow rate of 1.5 l/hour. Test temperatures were chosen as 1100, 1200 and 1300°C, so as to reproduce typical conditions prevailing in fibreglass making. Each sample was heated at a rate of 10°C/min up to the test temperature, then the experiment was carried out during 100 hours (except for some compositions which evidenced catastrophic oxidation). The time at which the test temperature was achieved was considered as the start of the thermogram.

After testing, the samples were cross sectioned, prepared for metallographic examination, observed by scanning electron microscopy and analysed by electron probe microanalysis.

3. Results

The influence of three main parameters on the oxidation behaviour of the alloys has been studied:

- Nature and content of the sintering agent used to produce homogeneous alloys
- Composition of the alloys (Cr content and Mo/W ratio)
- Temperature

As will be shown in the following sections, two types of oxidation kinetics were observed. The first one is characteristic of the formation of a Cr_2O_3 protective layer. Otherwise, a breakaway kinetics were correlated to the inability for the alloys to form a compact chromia scale. This type of behaviour involved the formation of complex oxides or volatilisation of refractory oxides.

3.1. Influence of the sintering agent

Referring to the good results obtained by Lee and Simkovich [3–6] with palladium as the sintering agent, this element was first selected to activate the sintering of chromium-rich alloys. According to Brophy *et al.* [8, 9] and Corti [10], nickel is also a very effective sintering agent, possibly even better than palladium. These two metals have thus been incorporated in increasing amounts to Mo-W-Cr alloys. To avoid any artifacts due to variation in the other alloy elements, all compositions tested had the same chromium content (39–40 wt%) and Mo/W weight ratio (equal to 1).

The influences of palladium and nickel on oxidation kinetics were studied at 1300°C, the highest temperature of the selected range, corresponding to more severe conditions.

The isothermal curves corresponding to the three compositions tested (40Cr-30Mo-30W, 39.5Cr-30Mo-30W-0.5Pd and 39Cr-30Mo-30W-1Pd) are presented in

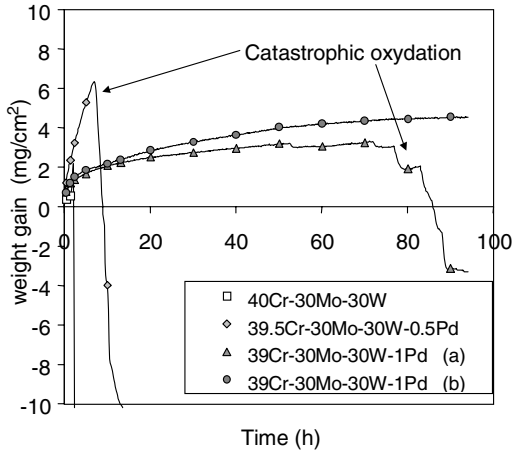

Figure 3 Isothermal oxidation curves of CrMoWPd alloys at 1300°C.

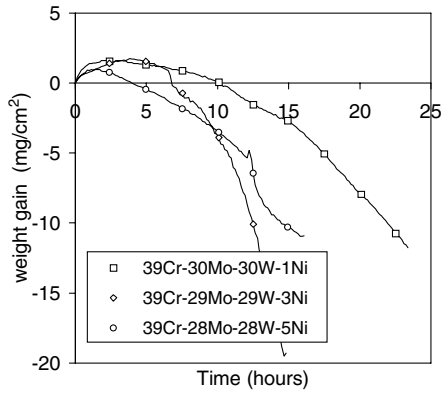

Figure 5 Isothermal oxidation curves at 1300°C of CrMoWNi alloys.

Fig. 3. The oxidation resistance of these alloys strongly depends on the palladium content. If the concentration of this element is lower than 1%, catastrophic oxidation occurs. The best results were observed for alloys containing 1 wt% Pd, however with poor reproducibility. For example, for the 39Cr-30Mo-30W-1Pd alloy, two types of behaviour was observed:

– a very slow oxidation rate with a total weight gain about 4mg/cm^2 after 100 hours testing (sample b),
– catastrophic oxidation after 60 hours at 1300°C (sample a).

The distribution of the elements in the 39Cr-30Mo-30W-1Pd alloy after testing (without breakaway) is shown on Fig. 4. An important chromium depletion was observed in the sample, since the chromium content at the surface decreased to 10 wt%. In the Cr depleted zone, which is as thick as 300 μm after 100 hours testing, palladium has been rejected from the initial solid solution into small precipitates mainly composed with Cr (80 at.%) and Pd (15%) as it was already demonstrated in a previous study [7].

The kinetics of oxidation at 1300°C for Cr-Mo-W alloys sintered with nickel are presented on Fig. 5. The three alloys tested (39Cr-30Mo-30W-1Ni, 39Cr-29Mo-29W-3Ni and 39Cr-28Mo-28W-5Ni) have quite similar oxidation behaviour. All curves show an important but regular weight loss due to vaporisation of volatile refractory oxides (MoO_3 and WO_3). Vaporisation seems however to be slower in the case of the alloy containing 1 wt% nickel.

The concentration profiles presented in Figs 6 and 7 show that, whatever the nickel content of the alloys, after about 20 hours oxidation, an important chromium depletion occurs at their surface. The thickness of the diffusion zone is about 30 μm.

Two different profiles can be observed, depending on the nickel content. With 1 wt% nickel, from inside the alloy towards the surface, the chromium concentration

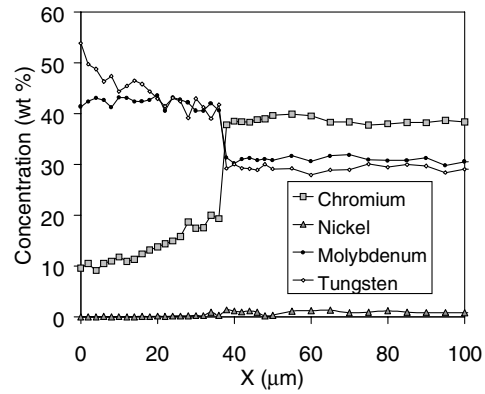

Figure 6 Concentration profile of the 39Cr-30Mo-30W-1Ni after 25 hours oxidation at 1300°C.

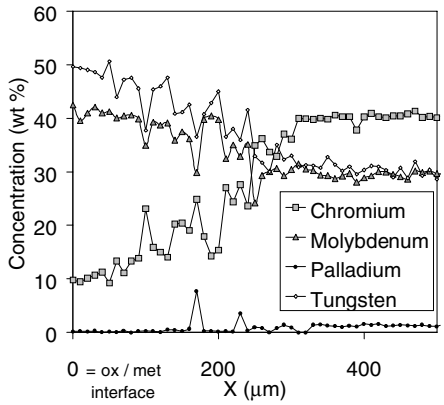

Figure 4 Electron probe microanalysis concentration profile of the 39Cr-30Mo-30W-1Pd alloy after 100 hours oxidation at 1300°C.

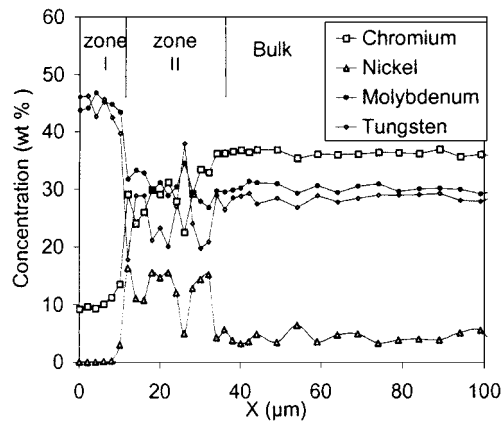

Figure 7 Concentration profile of the 39Cr-28Mo-28W-5Ni after 15 hours oxidation at 1300°C.

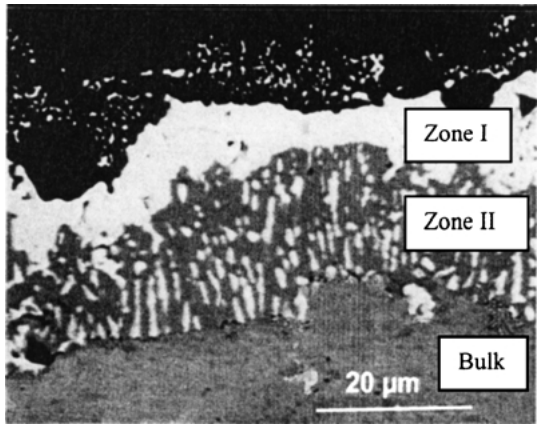

Figure 8 39Cr-28Mo-28W-5Ni alloy oxidised 15 h at 1300°C—back scattered electron (BSE) image.

drops sharply from 39 to 20 wt%, then decreases regularly from 20 wt% to 10 wt% (Fig. 6). For the alloys with 3 and 5 wt% nickel, two zones can be evidenced in the Cr depleted zone (Fig. 7 and Fig. 8). Zone II is composed of a α MoWCr with a low Cr content (about 10 wt% called phase 1) and of another phase containing all the elements of the alloy, but with a high nickel content (phase 2). The compositions of these two phases are given in Table II. Zone I, at the surface, comprises MoWCr without nickel.

For the oxide scale, contrary to the case of alloys containing palladium, no adherent nor compact protective scale is formed (Fig. 9). On the contrary it is a very porous mixture of Cr_2O_3 (dark) and $NiWO_4$(white).

3.2. Influence of the chromium content

The compositions of the Cr-Mo-W-Pd alloys oxidised at 1300°C are displayed in Table III Thermogravimetric curves are displayed in Fig. 10 with that of pure chromium, for comparison.

TABLE II Composition of the phases present in zone II formed during oxidation at 1300°C (39Cr-28Mo-28W-5Ni alloy)

Composition (wt%)	Cr	Mo	Ni	W
Phase 1	10.5	43.7	0.1	45.48
Phase 2	32.71	30.18	14.76	22.15

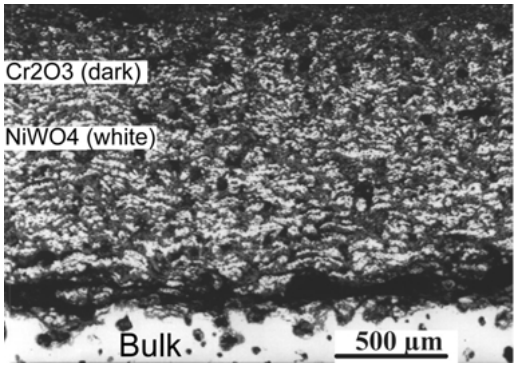

Figure 9 Cross-sectioned of the oxide formed on the 39Cr-28Mo-28W-5Ni alloy after 15 h at 1300°C (BSE image).

TABLE III Composition of the Cr-Mo-W-Pd alloys

Sample	Cr (wt%)	Mo (wt%)	Pd (wt%)	W (wt%)
S1	24	37.5	1	37.5
S2	29	35	1	35
S3	34	32.5	1	32.5
S4	39	30	1	30
S5	49	25	1	25

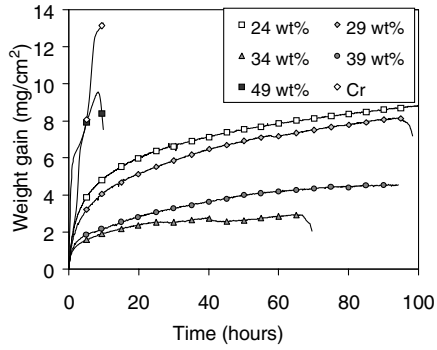

Figure 10 Isothermal oxidation curves of CrMoWPd alloys at 1300°C: influence of the chromium content.

According to their chromium content, the alloys exhibit different types of behaviours. The 49 wt% Cr alloy displays first a very high weight gain, similar to that of pure chromium. After about 10 hours, breakaway oxidation occurs, with evaporation of refractory metal oxides, and the weight of the samples decreases sharply. At least in the first step of their oxidation process, chromium-rich alloys behave like pure chromium with formation of a wrinkled, non-protective oxide, which spalls very easily. A thick and porous chromia scale forms, until the substrate is highly depleted with chromium; then Mo and W begin to oxidize and breakaway oxidation occurs.

The best behaviour is observed with 34 to 39 wt% Cr alloys. As can be seen on Fig. 10, their weight gain is low, corresponding to the growth of a compact and protective scale, as is shown on Fig. 11. On some samples however, oxidation breakaway occurs after less than one hundred hours, in the case of the 39 w% Cr alloy (see Fig. 3) and also for the 34 w% Cr alloy.

With chromium contents lower than 30%, the oxidation rate is higher, as can be seen in Fig. 10. The oxide

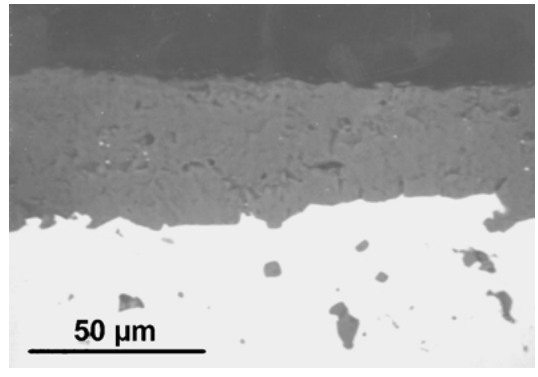

Figure 11 39Cr-30Mo-30W-1Pd alloy 100 h oxidation at 1300°C BSE image of the chromia scale.

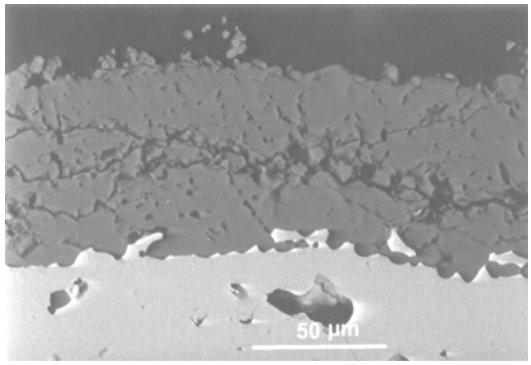

Figure 12 24Cr-37.5Mo-37.5W-1Pd alloy 100 h oxidation at 1300°C BSE image of the cracked and porous oxide.

layer is still chromia but, as can be seen in Fig. 12, it shows many cracks and is thus less protective than the scales formed on the 39 w% Cr alloys (Fig. 11). As for alloys with a high chromium level, oxidation breakaway can be observed.

3.3. Influence of the Mo/W ratio

The influence of the Mo/W ratio has been studied with alloys where the chromium and palladium contents had been fixed to 39% and 1%, respectively. The compositions prepared are given on Table IV.

In the case of tungsten-rich compositions, the technique of processing had to be modified, since in this case the conditions adopted for the majority of alloys led to heterogeneous samples. Thus the annealing time and temperature were increased to 50 h and 1600°C, to produce dense and homogeneous tungsten-rich alloys.

Fig. 13 shows weight gain vs time for the alloys tested. The best results are observed with alloys having a low molybdenum content. Molybdenum/Tungsten

TABLE IV Composition of the CrMoWPd alloys

Sample	Mo/W ratio	Cr (wt%)	Mo (wt%)	Pd (wt%)	W (wt%)
S6	3	39	45	1	15
S7	2	39	40	1	20
S8	1	39	30	1	30
S9	1/2	39	20	1	40
S10	1/3	39	15	1	45

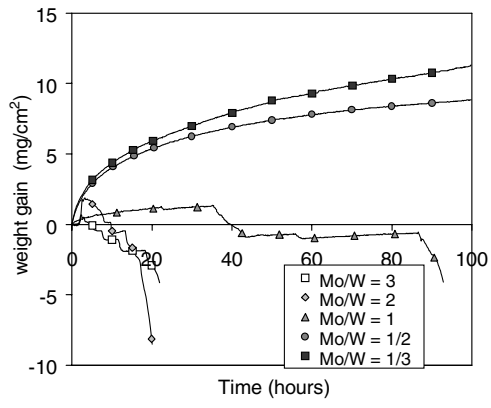

Figure 13 Isothermal oxidation curves of CrMoWPd alloys at 1300°C: influence of the Mo/W ratio.

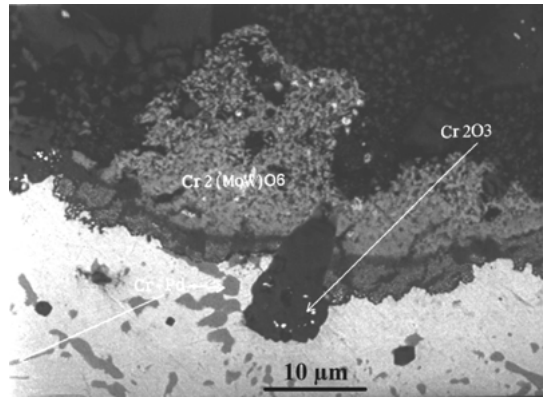

Figure 14 39Cr-45Mo-15W-1Pd—20 h at 1300°C BSE image.

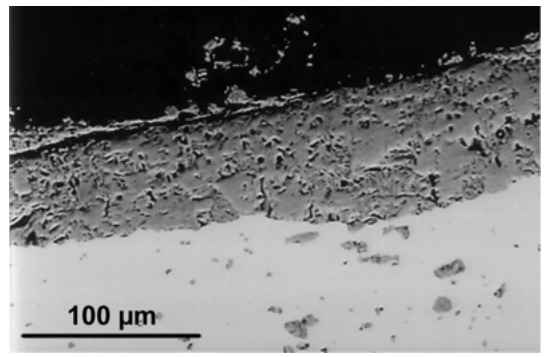

Figure 15 39Cr-15Mo-45W-1Pd—100 h at 1300°C BSE image.

ratios higher than 1 lead to catastrophic oxidation, with very high weight losses from the beginning of the tests. Observation of the metal-oxide interface shows that the oxide scale is non protective and contains two oxides identified as Cr_2O_3 and $Cr_2(WMo)O_6$ (Fig. 14). With Mo/W ratios lower than one no catastrophic oxidation is observed, at least for the duration of these experiments. The oxide scale formed in this case was compact (Fig. 15) but, as Fig. 13 shows, the weight gains measured for the two alloys tested are higher than that of the reference alloy (Mo/W = 1).

3.4. Influence of the temperature

The isothermal oxidation behaviour of the best three alloys selected (39%Cr, 1%Pd and Mo/W = 1, 1/2, 1/3) has been studied in a temperature range between 1100 and 1300°C (Figs 16–18).

As can be seen on Fig. 16, with 39Cr-30Mo-30W-1Pd alloy, no breakaway oxidation occurs at 1100°C and 1200°C. As mentioned before (Fig. 3), 1300°C seems to be a critical temperature, with some samples showing a good behaviour, whereas others are subjected to catastrophic oxidation after 50 to 100 hours.

Figs 17 and 18 show that no catastrophic oxidation occurs with W-rich alloys, whatever the temperature.

From the kinetic point of view, if oxide scale growth is governed by solid state diffusion, parabolic kinetics should be observed:

$$\frac{\mathrm{d}\left(\frac{\Delta m}{S}\right)}{\mathrm{d}t} = \frac{k'_p}{\frac{\Delta m}{S}} \qquad \text{(a)}$$

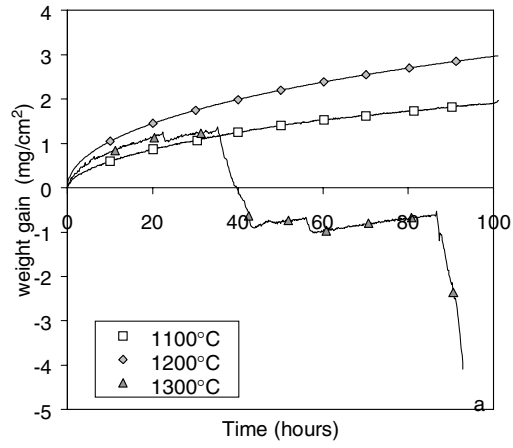

Figure 16 Isothermal oxidation curves of the 39Cr-30Mo-30W-1Pd alloy (Mo/W = 1): influence of the temperature.

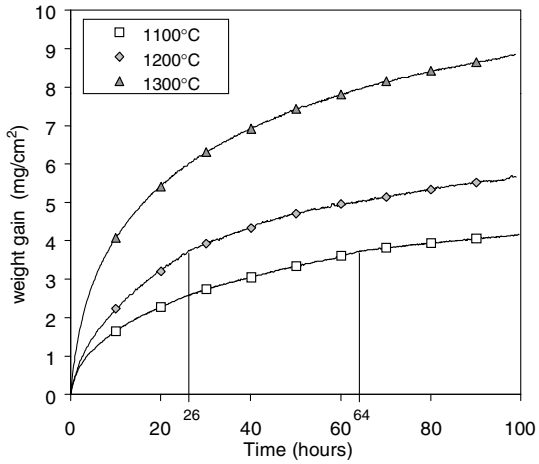

Figure 17 Isothermal oxidation curves of the 39Cr-20Mo-40W-1Pd alloy (Mo/W = 1/2): influence of the temperature.

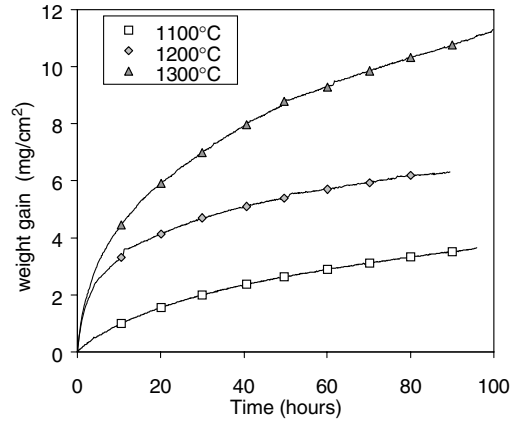

Figure 18 Isothermal oxidation curves of 39Cr-15Mo-45W-1Pd alloy (Mo/W = 1/3): influence of the temperature.

where $\frac{\Delta m}{S}$ is the weight gain ($g \cdot cm^{-2}$) and k'_p the parabolic constant

As mentioned by many authors [11, 12], volatilisation of chromia has to be taken into account at temperatures higher than 1000°C, with Cr^{VI} oxide formation via:

$$Cr_2O_3 + \frac{3}{2}O_2 \rightarrow 2CrO_3 \qquad (1)$$

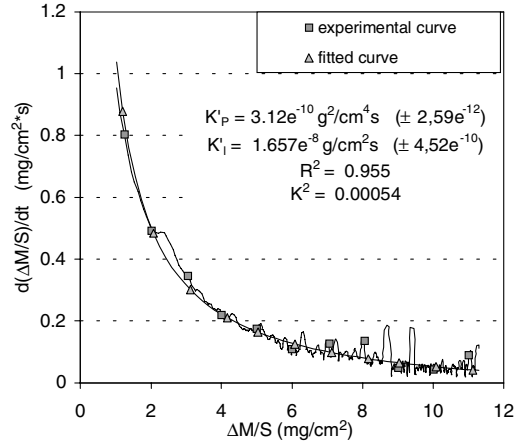

Figure 19 Fitted oxidation curve for the Mo/W = 1/3 alloy at 1300°C.

CrO_3 evaporation should be governed by linear kinetics:

$$\frac{d\left(\frac{\Delta m}{S}\right)}{dt} k'_l \qquad (b)$$

Where k'_l is the evaporation constant
The instantaneous weight gain rate is thus described by the Tedmon equation [13]

$$\frac{d\left(\frac{\Delta m}{S}\right)}{dt} \frac{k'_p}{\frac{\Delta m}{S}} - k'_l \qquad (c)$$

k'_p and k'_l can be determined by plotting the slope of the measured weight gain

$$\left(\frac{d\left(\frac{\Delta m}{S}\right)}{dt} f\left(\frac{\Delta m}{S}\right)\right)$$

curves vs the weight gain, then fitting the experimental curves to equation (c) by the least square method.

Numerical treatment was done using of the Microcal Origin software.† All calculations were done using this method on samples showing normal oxidation behaviour (no catastrophic oxidation). Illustration of the results obtained in the case where Mo/W = 1/3 is shown in Fig. 19. A few experiments have been duplicated. The recorded thermograms were similar and the result of the fit differ less than 20%. Thus, all oxidation rate constants and vaporisation constants are given with an error bar of 20%.

The results are reported in Fig. 20 where k'_p is shown as a function of $10^4/T$. For all the temperatures tested, MoW base chromia forming alloys exhibited a good oxidation behaviour from the kinetic point of view. Referring to the Hindam and Whittle diagram, the CrMoW alloys belong to the best chromia forming alloy.

Values of k'_p and k'_l as a function of the alloy composition have also been obtained for 1300°C. With Mo/W fixed to 1, k'_p and k'_l decreased with increasing Cr content, from 24 to 39% (Fig. 21). This is in agreement

†Microcal ™

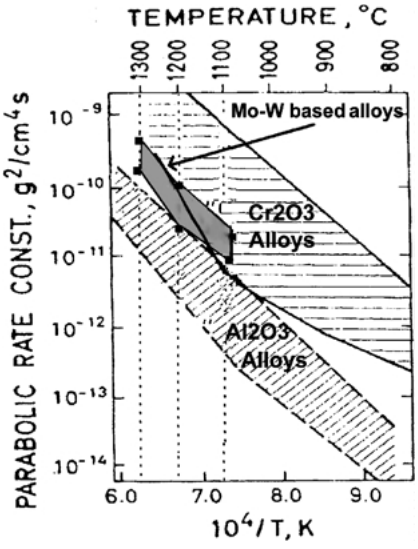

Figure 20 Calculated rate constant of chromia former Mo-W based alloys compared with Cr_2O_3 and Al_2O_3 former alloys, referring to Hindam and Whittle [14].

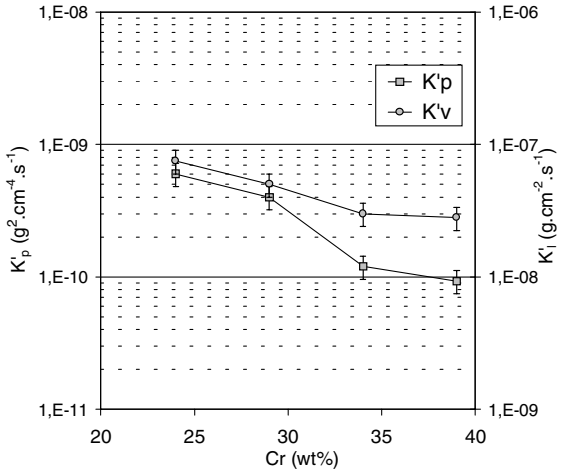

Figure 21 Evolution of the rate and vaporisation constants with the chromium content.

with the observations of the oxide scale morphology. Figs 11 and 12 show indeed that the chromia scale is more porous when the chromium content of the alloy is low.

Dependence of the kinetic constants versus Mo/W ratio and temperature have also been determined. The results are presented on Figs 22 and 23. As regards K'_p, the Mo/W = 1 alloy (39Cr-30Mo-30W-1Pd) evidences a very low value whatever the temperature, as compared to the other two compositions studied. This kinetic result is confirmed by thickness measurements of the oxide scale.

No clear tendency can be deduced for the dependence of K'_l on temperature for the alloys tested (Fig. 23), except the similar behaviour of pure chromia and Mo/W = 1 alloy.

From the morphological point of view, some differences were observed for oxide scales and bulk alloys, which can give informations on the differences observed between the kinetic regimes of the three alloys tested.

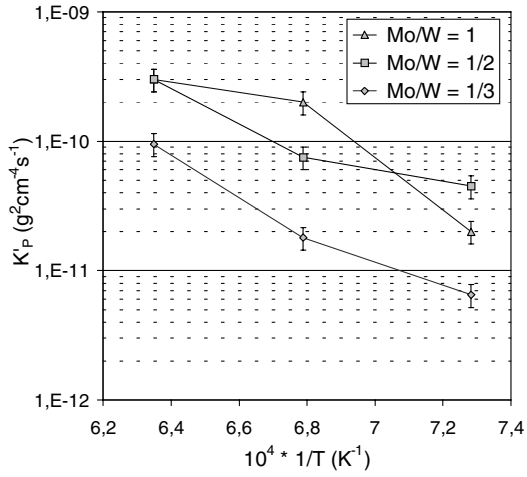

Figure 22 Evolution of the rate constant with the temperature and the Mo/W ratio.

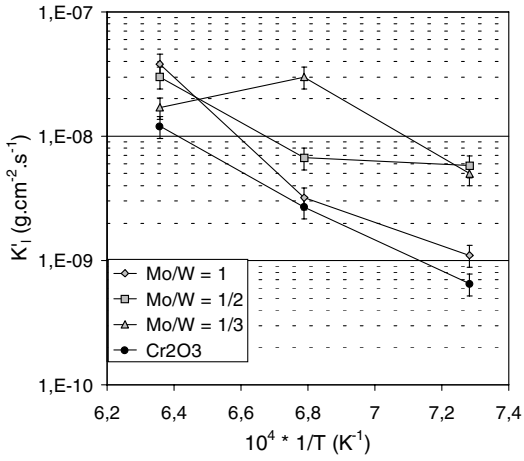

Figure 23 Evolution of the vaporisation constant with the temperature and the Mo/W ratio.

With Mo/W = 1/2 alloy, two oxidation regimes are observed at 1100 and 1200°C. The first one corresponds to initial growth of a two-phase oxide scale mainly constituted with chromia, containing a small quantity of Cr_2WO_6 (Fig. 24). The second one corresponds to pure chromia scale growth (Fig. 25).

The transition time between these two regimes decreases with temperature. At 1300°C, only the second

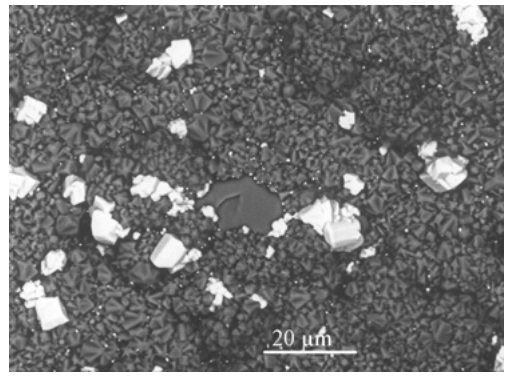

Figure 24 Back scattered micrography of the surface of the oxide formed 39Cr-20Mo-40W-1Pd at 1200°C before the transition time: the two oxides Cr_2WO_6 (white) and Cr_2O_3 (grey) are easily observed. Cracks and holes can also be seen in the chromia layer.

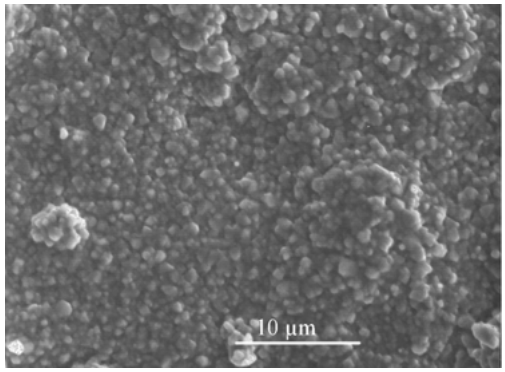

Figure 25 Scanning electron micrography of the surface of the oxide formed 39Cr-20Mo-40W-1Pd at 1200°C after the transition time: the oxide layer is composed of Cr_2O_3 and no crack is observed.

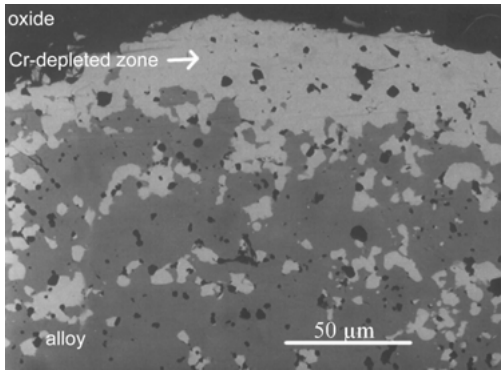

Figure 26 Back scattered micrograph of the 39Cr-15Mo-45W-1Pd alloys after oxidation experiment at 1300°C two phases are observed: a chromium phase (grey) and a tungsten phase (white), with the same composition of the Cr-depleted zone.

oxidation regime is observed, and no transitory phase like Cr_2WO_6 can be observed.

With Mo/W = 1 and Mo/W = 1/3, formation of Cr_2WO_6 is not observed, whatever the oxidation temperature. This could seem surprising for Mo/W = 1/3 alloy, which has a very high tungsten content. The structure of the alloy is however significantly different in this case, as Fig. 26 shows. The bulk alloy is two-phased, with tungsten-rich precipitates dispersed in a chromium rich matrix. Near the oxide scale, chromium depletion leads to tungsten segregation with formation of a monophase scale.

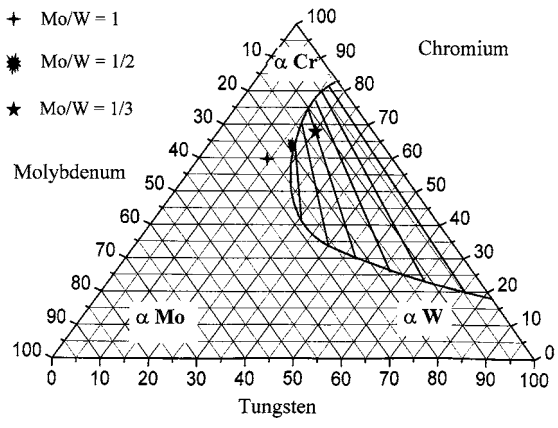

Figure 27 Ternary phase diagram of the Cr-Mo-W system at 1300°C: at.% [15].

Partial determination of the ternary MoWCr phase diagram at 1300°C show that the figurative point corresponding to Mo/W = 1/3 alloy is located in the two phase domain of the ternary system. This result is in accordance with the ternary phase diagram witch isothermal section for 1300°C is given in Fig. 27.

4. Discussion

The oxidation resistance of Mo/W base, chromia forming alloys, was conditioned by their ability to form a dense, protective, chromia scale, depending mainly on the chromium diffusion flux from the bulk alloy towards the surface. If this flux is too low to sustain the growth of chromia, then molybdenum and/or tungsten oxides can form and induce catastrophic oxidation, as observed previously by Evans on WCrPd alloys [1], also by Lee and Simkovich on Mo-Cr-Pd and W-Mo-Cr-Pd alloys [3–6].

Volume diffusion of chromium through alloy grains is not very rapid, since molydenum and tungsten are refractory metals, with very high melting points. The maximum oxidation temperature studied (1300°C) is indeed approximately half the melting point of the base alloy (0.5 T_f), which is generally considered as the value above which volume diffusion becomes significant. This point is confirmed by the results obtained in the study done on preparation of these alloys by sintering [7]: no dense alloys can be obtained if activating agents (Ni or Pd) are not used.

Nickel seems to affect chromium diffusion only during sintering since alloys containing this element show a catastrophic oxidation behaviour, whatever the nickel content of the alloys. For palladium, two types of behaviour can be observed, following its concentration in the alloys. If it is lower than 1 wt%, catastrophic oxidation occurs very rapidly. As for nickel, it can be supposed that palladium, when present at low level, dissolves in the alloy matrix without significant modification of its bulk diffusion coefficients. If the palladium content is higher than 1wt%, good oxidation properties can be observed for alloys containing 24 to 39 wt% chromium, although in some cases, catastrophic oxidation occurs after some tenths of hours at 1300°C. With chromium contents lower than 34 wt% or higher than 39 wt%, no satisfactory behaviour can be observed during oxidation tests.

With MoWCrPd alloys containing 1 wt% palladium, there is a correlation between the Cr/Pd ratio and the oxidation behaviour. This can be explained by the dependence of the palladium solubility and of the activity of chromium in the matrix, with the composition of the alloy. With 39 wt% Cr or less, the solubility limit of palladium in the alloys at 1300°C is probably less than 1 wt%: α CrPd phase thus precipitates in the grain boundaries, enhancing the chromium diffusion rate. Moreover, depletion of chromium near the oxide scale, consecutive to chromia formation, must lead to segregation of a palladium-rich phase containing chromium at this interface, as mentioned previously by Evans [1]. Molybdenum and tungsten have a very low solubility in palladium: their diffusion fluxes

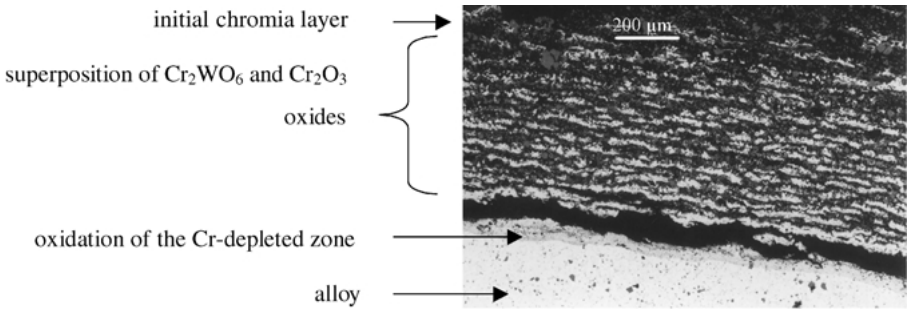

Figure 28 Morphology of the oxide scale formed during catastrophic oxidation.

towards the surface are thus very low and only chromia can form.

If the chromium concentration of the alloy is lower than 30 wt%, the chromia scale is less protective (Figs 10–12). This can be explained by considering that the lower chromium activity in the alloy induces a lower diffusion rate of this element, especially because the grain size of the alloys is inversely proportional to their chromium content [7]. This study evidences that a low Cr content leads to high grain size and that Cr diffusion occurs essentially at the grain boundaries. Consequently, for these two reasons, a high chromium content improve the chromia forming scale. Limited oxidation of molybdenum and tungsten can thus occur, contributing to enhance the porosity of the chromia scale.

With chromium contents higher than 39 wt%, palladium is completely dissolved in the alloy matrix. No CrPd can form and the chromium rich alloys thus behave like pure chromium: wrinkled, non protective chromia scale form and catastrophic oxidation occurs after some hours at 1300°C.

Catastrophic oxidation observed at 1300°C with alloys sintered with Ni or Pd at low concentration (<1 wt%), can be described by referring to previous work done by Lee and Simkovich [3] who studied the oxidation mechanism of Cr-W-Pd alloys. These authors have shown that several oxides form at the beginning of the experiments. In the initial stage, the alloy surface is covered with WO_3, Cr_2WO_6 and Cr_2O_3, the volume fraction of WO_3 and Cr_2WO_6 being correlated to the tungsten content of the alloys. If protective chromia cannot form, for the reasons stated previously, the oxide scale growth is very rapid, since as Fig. 28 shows that this scale is constituted with a mixture of chromia and mixed oxides like Cr_2WO_6.

Formation of Cr_2WO_6 during the first steps of oxidation can explain why, at constant temperature, the weight gain increases with the tungsten content in the case of alloys containing 1 wt% Pd (Fig. 22). As mentioned before, the volume fraction of Cr_2WO_6 is higher on tungsten rich alloys, thus explaining the differences between time for transition for the two oxidation regimes: mixed oxide scale and pure chromia scale growth. During the second kinetic regime, Cr_2WO_6 should decompose following the equation :

$$Cr_2WO_6(s) \Rightarrow Cr_2O_3(s) + WO_3(g) \qquad (2)$$

The thickness of the oxide scale formed on tungsten rich alloys should thus increase.

Relevant to the influence of the temperature on the oxidation behaviour of Mo-W-Cr-Pd alloys, from Figs 16 to 18, catastrophic oxidation is observed only at 1300°C, in our experiments. At 1200°C and especially at 1100°C, chromium depletion of the alloy is lower, since the rate of growth of chromia is significantly lower.

5. Conclusion

The oxidation behaviour of CrMoW alloys has been investigated over a broad range of compositions. Syntheses of these materials were carried out by pressure sintering and with use of two sintering agents, palladium and nickel. From these two additives, only palladium has a significant influence on the oxidation behaviour of the MoWCr alloys. When present at a high enough concentration, this element is rejected at the grain boundaries allowing a fast diffusion of chromium towards the surface. As regards nickel, this metal is a good sintering agent but it does not improve the oxidation behaviour since it is soluble in the alloy.

Study of the influence of the content of major elements on the behaviour of Pd-sintered alloys have shown that increasing the chromium content increases the oxidation resistance of the alloy up to a maximum value corresponding approximately to 40 wt%. Above this value, catastrophic oxidation occurs since, first palladium dissolves totally in the matrix of the alloys and second the alloys properties are nearer those of pure chromium than those of refractory metals base alloys.

The best oxidation properties are observed for high tungsten concentration. Comparison of the calculated parabolic rates constant of these alloys with those of typical alumina and chromia forming alloys show that they show an oxidation resistance near from that of the best alumina forming alloys.

References

1. D. S. EVANS, in High Temperature Materials, 6th Plansee Seminar, Metallwerk Plansee, Austria, 1968, p. 42.
2. I. YA. DZYKOVICH, V. V. PANICHKINA, V. V. SKOROKHOD and L. I. SHAIDERMAN, *Poroshk. Metall.* **2**(158) (1976) 86.
3. D. LEE and G. SIMKOVICH, *Oxid. Met.* **34**(1/2) (1990) 13.
4. *Idem.*, *ibid.* **31**(3/4) (1989) 265.
5. *Idem.*, *J. Less-Com. Met.* **163** (1990) 51.
6. *Idem.*, *ibid.* **169** (1991) 19.
7. S. DILIBERTO, O. KESSLER, C. RAPIN, P. STEINMETZ and P. BERTHOD, *J. Mater. Sci.* **37** (2002) 3277.

8. H. W. HAYDEN and J. H. BROPHY, *J. Electrochem. Soc.* **110**(7) (1963) 805.
9. J. H. BROPHY, L. A. SHEPARD and J. WULFF, in "Powder metallurgy," edited by W. Leszinski (AIME-MPI, Interscience, New York, 1961) p. 113.
10. C. W. CORTI, *Plat. Met. Rev.* **30**(4) (1986) 184.
11. C. WAGNER, *Z. Physik. Chem.* B **21** (1933).
12. P. KOFSTAD, in "High Temperature Corrosion" (Elsevier Applied Science, 1988).
13. C. S. TEDMON, *J. Electrochem Soc.* **113**(8) (1966) 766.
14. H. HINDAM and D. P. WHITTLE, *Oxid Met.* **18**(5/6) (1982) 245.
15. "Ternary Equilibrium Diagrams," 2nd ed. Chapman and Hall (London, 1982) p. 9065.

Received 12 June 2001
and accepted 29 October 2002